HHS Public Access

Author manuscript

Nanoscale. Author manuscript; available in PMC 2016 June 14.

Published in final edited form as:

Nanoscale. 2015 June 14; 7(22): 10085–10093. doi:10.1039/c5nr01857a.

Toxicity and Oxidative Stress Induced by Semiconducting Polymer Dots in RAW264.7 Mouse Macrophages

Fangmao Ye[#1], **Collin C. White**[#2], **Yuhui Jin**[3], **Xiaoge Hu**[4], **Sarah Hayden**[1], **Xuanjun Zhang**[1], **Xiaohu Gao**[4], **Terrance J. Kavanagh**[2,*], and **Daniel T. Chiu**[1,*]

[1] Departments of Chemistry, University of Washington, Seattle, WA 98195 (USA)

[2] Department of Environmental and Occupational Health Sciences, University of Washington, Seattle, WA 98195 (USA)

[3] Corning Incorporated, Corning, NY, 14831 (USA)

[4] Department of Bioengineering, University of Washington, Seattle, WA 98195 (USA)

[#] These authors contributed equally to this work.

Abstract

The rapid development and acceptance of PDots for biological applications depends on an in depth understanding of their cytotoxicity. In this paper, we performed a comprehensive study of PDot cytotoxicity at both the gross cell effect level (such as cell viability, proliferation and necrosis) and more subtle effects (such as redox stress) on RAW264.7 cells, a murine macrophage cell line with high relevance to in vivo nanoparticle disposition. The redox stress measurements assessed were inner mitochondrial membrane lipid peroxidation (nonyl-acridine orange, NAO), total thiol level (monobromobimane, MBB), and pyridine nucleotide redox status (NAD(P)H autofluorescence). Because of the extensive work already performed with QDots on nanotoxicity and also because of their comparable size, QDots were chosen as a comparison/reference nanoparticle for this study. The results showed that PDots exhibit cytotoxic effects to a much lesser degree than their inorganic analogue (QDots) and are much brighter, allowing for much lower concentrations to be used in various biological applications. In addition, at lower dose levels (2.5 nM to 10 nM) PDot treatment resulted in higher total thiol level than those found with QDots. At higher dose levels (20 nM to 40 nM) QDots caused significantly higher thiol levels in RAW264.7 cells, than was seen with PDots, suggesting that QDots elicit compensation to oxidative stress by upregulating GSH synthesis. At the higher concentrations of QDots, NAD(P)H levels showed an initial depletion, then repletion to a level that was greater than vehicle controls. PDots showed a similar trend but this was not statistically significant. Because PDots elicit less oxidative stress and cytotoxicity at low concentrations than QDots, and because they exhibit superior fluorescence at these low concentrations, PDots are predicted to have enhanced utility in biomedical applications.

[*] Corresponding authors: ; Email: tjkav@u.washington.edu, ; Email: chiu@chem.washington.edu

Introduction

Semiconducting polymer dots (PDots) have recently emerged as a new group of fluorescent probes which possess large absorption cross-sections, high quantum yields, and fast emission rates[1-8]. The brightness of PDots has been shown to be an order of magnitude higher than that of quantum dots (Qdots) and three orders of magnitude higher than organic dyes[5,9]. These properties of PDots make them excellent fluorescent probes for many biological applications. For example, they recently have been used for biological detection and imaging [1,9-12] biosensing platforms[13,14], specific cellular[5] and subcellular targeting and imaging[15], photoacoustic molecular imaging probes[16], drug delivery[17], bioorthogonal labeling[6] and *in vivo* tumor targeting[9,18].

In order to further promote PDots for the biological uses, especially *in vivo* applications, a comprehensive understanding of PDot cytotoxicity is of great significance because biocompatibility is an extremely important consideration for fluorescent nanoparticles aimed at biological applications. Indeed, there have been a few studies[10,19-21,22] recently published related to PDot cytotoxicity. For example, Christensen and co-workers evaluated the possible cytotoxic effects of hydrophobic PDots with a size of 18 nm[10] by assessing the viability of cells incubated with increasing amounts of PDots using Cell Titer Blue, a dye that tracks cell viability and proliferation. The result showed that the percentage of live J774A1 cells after an 18 hour incubation with PDots was indistinguishable from the control at all concentrations tested. Li and coworker[22] conducted proliferation studies of blue-emitting PDHF PDots on human gastric adenocarcinoma (SGC-7901) cells and human gastric mucosal (GES-1) cells. They also evaluated PDot cytotoxicity based on their ability to cause reactive oxygen species (ROS) generation and changes in mitochondrial membrane potential (MMP). Their results indicated that PDots promoted cell growth by slightly increasing intracellular ROS (consistent with a mitogenic signal) and by modulating MMP. However, the depth and breadth of these studies[10,19-21,22] has been fairly limited. In this paper, we present a much more in-depth look at the toxicological effects of PDots, which not only includes gross effects on cells, but also the more subtle effects (such as redox stress) on RAW264.7 cells based on the measurements of inner mitochondrial membrane lipid peroxidation, total thiol levels, and pyridine nucleotide autofluorescence. RAW264.7 cells, a commonly used murine macrophages cell line, was chosen as a highly relevant cell for PDots because these nanoparticles will most likely come in contact with various macrophages (alveolar, liver, spleen, lymph nodes) during *in vivo* exposures. Additionally, because of the extensive work[23-25] already performed regarding the nanoparticle toxicity of polymer-coated Qdots, and also because they have comparable size to PDots (dye-loaded polystyrene beads are too large, and we use PDots of about same size as QDots), we chose QDots as a comparison/reference nanoparticle for this study. It should be noted that all the studies performed in this work are short term, most within 24 hr of initial exposure. Therefore, there should not be any leakage of heavy metal from the amphiphilic polymer-coated QDots. We demonstrated that PDots exhibit cytotoxic effects to a much lesser degree than their inorganic analogous nanoparticle and are much brighter, allowing for much lower concentrations to be used in biomedical applications.

Materials

Poly[(9,9-dioctylfluorenyl-2,7-diyl)-co-(1,4-benzo-{2,1',3}-thiadiazole)] (PFBT, MW 157,000, polydispersity 3.0), were purchased from ADS Dyes, Inc. (Quebec, Canada). TOPO QDots (TOPO coated CdSe/ZnS core/shell QDots) were purchased from Ocean Nanotech. The polymer poly(styrene-co-maleic anhydride) (PSMA, average Mn ~1,700, styrene content 68%) was purchased from Sigma-Aldrich (St. Louis, MO, USA)). All other reagents for Pdot and Qdot preparation were purchased from Sigma-Aldrich (St. Louis, MO, USA). The RAW264.7 mouse macrophage cell line was obtained from the American Type Culture Collection (ATCC, Manassas, VA).

Methods

Preparation of PFBT, PFBT/PF-DBT5, and PFBT/NIR720 PDots

PDots were prepared using a nanoscale reprecipitation technique[5,9]. 1. For green PFBT PDots, a tetrahydrofuran (THF) solution containing 100 μg/mL of PFBT and 20 μg/mL poly(styrene-co-maleic anhydride) (PSMA) was prepared. 2. Red PFBT/PF-DBT5 PDots were prepared from a THF solution containing 70 μg/mL of poly[(9,9-dioctylfluorenyl-2,7-diyl)-co-(1,4-benzo-(2,1',3)-thiadiazole)] (PFBT), 30 μg/mL poly(9,9-dioctylfluorene)-co-(4,7-di-2-thienyl-2,1,3-benzothiadiazole) (PF-DBT5)[9], and 20 μg/mL PSMA. 3. NIR PFBT/NIR720 PDots was prepared from the THF solution contained 90 μg/mL of PFBT, 10 μg/mL of NIR720 dye, and 20 μg/mL PSMA. The structures of PFBT, PF-DBT5 and NIR720 are shown in Figure 1. A 5 mL aliquot of the above mentioned mixture solution was then quickly dispersed into 10 mL of water under vigorous sonication. The THF was then evaporated at an elevated temperature (not exceeding 100 °C) under the protection of nitrogen gas. The THF-free PDot solutions were filtered through a 0.2 μm cellulose membrane filter and concentrated to 1 μM using Millipore Amicon Ultra (100 kDa) centrifugal filter tubes. The PDots were stable in several buffers that we tested, including TRIS, TBE, PBS, and HEPES, without showing any size change for up to 6 months of storage at 4 °C.

Preparation of amphiphilic polymer-coated TOPO-PMAT CdSe/ZnS QDots

Amphiphilic polymer coated TOPO-PMAT CdSe/ZnS QDots were prepared as previously reported[23,24]. Briefly, 40 mg of PMAT was mixed with 17.7 nmol of TOPO QDots suspended in chloroform. The solvent was then allowed to evaporate, leaving a thin film of TOPO-PMAT QD complexes. The complexes were dissolved in 50 mM borate buffer (pH 8.5) using agitation or sonication. Any unbound PMAT polymer was removed by ultracentrifugation.

Cell Culture

RAW264.7 mouse macrophages were grown to ~80% confluence in RPMI 1640 medium supplemented with L-glutamine, phenol red, 10% fetal bovine serum, 100 IU/ml penicillin, 100 ug/ml streptomycin, 100 mM HEPES, and 1.5 mM sodium pyruvate at 37 °C in humidified air containing 5% CO_2.

QDot and PDot Treatments

QDots and PDots were added to complete cell culture medium and then passed through a 0.2 um filter before exposure to the cells. RAW264.7 cells were treated with 0, 2.5, 5, 10, 20 or 40 nM QDots or PDots for 24 hr. After exposure all cells were rinsed 2X with PBS and released from plates with No-Zyme (Sigma-Aldrich, St. Louis, MO) and then subjected to staining protocols.

MTT Cell Viability Assay

RAW264.7 cells were added to a 96-well plate at 20,000 cells/ well and allowed to attach to the plate overnight. In each plate, cells were treated in triplicate for 24 h with either PDots, distilled water (dH_2O; vehicle control) or 0.2 nM etoposide (positive control). Five μL of MTT stock solution (5 mg/mL), was added to each well in 100 μL of medium. The plates were gently shaken by hand for 5 min and then placed back into the cell culture incubator for 20 min. Medium was completely aspirated from each well taking care not to disturb the cell layer. Next, 150 μL of dimethyl sulfoxide (DMSO) were added to solubilize the formazan dye and the plates were rocked for 5 min. A 100 μL aliquot of the DMSO/ formazan solution was then transferred to another 96 well plate, and absorbance was measured at 570 nm on a Multiskan Spectrum UV/visible Microplate Reader (Thermo Labsystems, Waltham, MA).

Trypan Blue Viability Assay and Cell Counts

The setup for the Trypan Blue viability assay and cell counts was performed as for the MTT assays. After the 24 h incubation period with PDots, Trypan Blue solution (0.4%) was added as 1% of the final volume of the well. Cells were detached from the wells by serial trituration and a 10 μL volume of the cell suspension was placed on a hemacytometer for counting of viable (unstained), dead (stained), and total cell count.

Cell Cycle Analysis by Flow Cytometry

RAW264.7 cells were plated at 50,000 cells per well in 6-well plates and allowed to attach overnight. Cells were treated in triplicate for 24 h with concentrated red PDots for a final concentration of 24 nM, or with vehicle (dH_2O) or positive (0.2 nM etoposide) controls. Cells were harvested, placed in 15 mL tubes and centrifuged at 800 rpm for 5 min. Medium was aspirated and the cell pellet was resuspended in 500 μL cold calcium and magnesium-free phosphate buffered saline (CMF-PBS). The cell suspension was added drop-wise to centrifuge tubes containing 4.5 mL of ice cold 70% ethanol while vortexing, and stored on ice until all samples were completed. Samples were covered and kept in a cold room overnight. Samples were then centrifuged at 800 rpm for 5 min and the supernatant was aspirated. Cells were resuspended in 500 μL of propidium iodide staining buffer (propidium iodide, 5 ug/mL; RNAse, 0.1 mg/mL; 0.1% Triton X-100 in CMF-PBS). Samples were then analyzed on a flow cytometer (ALTRA, Beckman-Coulter, Miami, FL), with excitation at 488 nm and PI fluorescence emission collected with a 620/30 band pass filter. A minimum of 10,000 cells were collected for each sample.

Measures of Qdot and Pdot Uptake, Toxicity and Oxidative Stress by Flow Cytometry

Fluorescent indicators of toxicity and oxidative stress included nonyl-acridine orange (NAO; oxidized cardiolipin in the inner mitochondrial membrane), monobromobimane (MBB; total thiols), Hoechst 33258 (necrosis) and UV-induced blue autofluorescence (NAD(P)H). Subsequent to treatment, 10^6 Raw264.7 cells were incubated with either 10 uM MBB plus 2 mM probenicid for 10 min, 0.1 ug/ml NAO plus 2 mM probenicid for 15 min, or 2 ug/ml Hoechst at 37 °C. After incubation, stained cells were placed on ice prior to flow cytometry analysis.

Flow Cytometry

PDot or QDot uptake, MBB, NAO, Hoechst and NAD(P)H fluorescence were analyzed on a Beckman-Coulter ALTRA flow cytometer. UV (351-365 nm) excitation, and a 450/35 nm BP filter were used for MBB, Hoechst or NAD(P)H emission detection. Excitation for NAO was at 488 nm, and emission was detected using a 525/40 nm BP filter. For QDot and PDot fluorescence, excitation was at 488 nm and emission was collected with a 620/30 nm BP filter. A total of 10,000 cells were analyzed per sample. Beckman/Coulter Expo32 software was used to analyze flow cytometry data. Two-way ANOVA and a Student T test on dose and particle effects were performed in Excel (Microsoft, Redmond, WA).

Measure of Colocalization by Image Cytometry

PDots and QDots treatments: RAW264.7 cells were grown to 70% confluence in coverslip chamber slides (Nunc™ Lab-Tek™). Medium was removed and cells were then exposed for 1 hr to either 2.5 nm QDots or 2.5 nm PDots suspended in RPMI medium (both filtered through a 0.2 um filter). After exposure all cells were rinsed 2X with PBS for 5 min and then taken through the intracellular organelle staining protocols.

Fluorescent Stains for Organelles

Stains or antibodies used were Lamp1 (lysosomes), early endosomal antigen1 (EEA1; early endosomes), Mitotracker green (mitochondria), and NBD C6-ceramide complexed to BSA (Golgi). For mitochondrial staining, cells were incubated in RPMI with 40 nM Mitotracker green for 30 minutes in a cell culture incubator then rinsed 2X with RPMI for 5 min. For staining of lysosomes, cell were rinsed twice in PBS for 5 min and fixed with 5% PFA (paraformaldehyde) for 15 min at room temperature followed by blocking and cell penetration for 30 min with PBS/1% BSA/0.1% Sodium azide/1% Saponin (PBSS). Following the blocking step the cells were incubated for an additional 30 min in 0.5 ug/ml Lamp 1/PBSS and washed 2X in PBS. For early endosomal staining, cells were fixed as for Lamp 1, blocked and penetrated for 30 min with PBSS and 5% goat serum. Cells were then incubated for 30 min in EEA1 at 0.5 ug/ml in PBSS, washed with PBS and incubated an additional 30 min in rabbit-anti goat IgG Alexa 488 at 5 ug/ml in PBSS. For Golgi stain, cells were washed for 5 min with HBSS/10mM HEPES followed by a 30 min incubation in 100 ul 5 uM NBD C6 ceramide/BSA complex/400 ul HBSS/10 mM HEPES per well at 4 °C. Cells were then rinsed 2X in HBSS/10mM HEPES followed by an additional 30 min incubation in HBSS/HEPES in a cell culture incubator. Cells were then subjected to confocal imaging as soon as possible after all staining procedures.

Confocal imaging of PDots and QDots and organelles

Confocal images were taken with a LSM510 scanning confocal microscope (Zeiss, Thornwood, NY). Laser excitation was at 488 nm and for fluorescence emission detection, a 520/40 BP filter (all organelle stains) and a 620/20 BP filter (QDots or PDots) were utilized. Colocalization of QDots and PDots with organelles was undertaken using Metamorph image analysis program (Molecular Devices, Sunnyvale, CA).

Results and Discussion

1. Comparison of PDots and QDots properties in particle form

Three PDots with emission ranging from green (PFBT), red (PFBT/PF-DBT5), and NIR (PFBT/NIR720) were synthesized and used in this study. All three PDots were investigated with respect to cell membrane integrity and mitochondrial dehydrogenase activity as a measure of cell viability and growth using the Trypan Blue and MTT assays, respectively. In order to perform a fair comparison between PDots and QDots in terms of cellular uptake, mitochondrial cardiolipin peroxidation, total thiol levels, necrosis/membrane integrity and reduced pyridine nucleotides, only red PFBT/ PF-DBT5 PDots was used. The reason for this was that among the three PDots investigated using the same excitation source (488nm), the red PDots have the closest emission peak to that of the amphiphilic polymer coated QDots. It should be noted that the zeta potential of these three Pdots was measured to be −45mV, while the zeta potential of Qdot was measured to be −43 mV.

Figure 1, panels A and B, show the respective route used to prepare PDots and Qdots, as well as schematic of their structural design. Both PDots and QDots had carboxylic acid groups on their surface. The hydrodynamic diameter for PDots and QDots as determined by DLS was 16 nm and 13 nm, respectively. PDots showed an absorption peak at 460 nm and a fluorescence emission peak located at 630 nm (panel C), while QDots showed decreasing absorbance towards longer wavelengths and a fluorescence emission peak located at 620 nm (panel D). The bandpass filter used in the flow cytometry experiment was 620/30, which is slightly more favorable for QDots than for PDots. The quantum yield for PDots and QDots was reported to be 56%[9] and 45%, respectively.

2. Cellular uptake of PDots and QDots as measured by mean fluorescence intensity

The murine macrophage cell line RAW264.7 was selected for the these studies since these nanoparticles would most likely come in contact with macrophages in various physiological locations (alveolus, liver, spleen, lymph nodes, etc.) with *in vivo* exposures. RAW264.7 cells were previously reported to show good uptake capability for QDots[24]. In this study, RAW264.7 cells avidly took up both QDots and PDots as shown in Figure 2. Cells that uptaked Pdots showed an apparent higher fluorescence intensity than those that uptaked QDots at similar biologically relevant dosing concentrations. For example, at 10 nM level, the cellular uptake (i.e. mean fluorescence intensity) for PDots is 10 times higher than that of QDots. However, the differences in fluorescence intensity between PDots and QDots could be due to either differences in uptake, or more likely due to the higher brightness of PDots relative to that of QDots[5]. Nevertheless, the uptake results using flow cytometry indicated that the endocytosis of PDots into RAW264.7 cell is very efficient.

3. Cell viability study by MTT and Trypan Blue assays

The acute toxic effects of nanoparticle on cells, including proliferation and viability, are often determined by MTT reduction (a yellow tetrazole, which is reduced to purple formazan in living cells) and Trypan Blue exclusion (a diazo dye, which is used to probe cell membrane integrity). We performed these two assays for all three PDots types with different emission wavelengths. The results are shown in Figure 3, panel A (MTT reduction) and panel B (Trypan Blue exclusion). The viability of treated cells is calculated as a percentage the viability of cells treated with vehicle only. The MTT viability assay (Figure 3 panel A) showed a very light decrease (less than 8%) as the dose increased for all three PDots. The positive control (0.2 nM Etoposide) showed an 80% decrease in cell viability. There was essentially no change in cell membrane integrity using Trypan Blue for all three PDots (Figure 3, panel B), while the positive control with 0.2nM Etoposide showed a 30% decrease. These results indicated that PDots do not substantially affect cell viability for doses ranging from 2.5 nM to 40 nM, which is consistent with previously reported results[10,19–21,22] and are comparable to those of QDots previously reported as well[24].

4. Necrosis/membrane integrity by Hoechst 33342 fluorescence

Necrosis refers to passive, accidental cell death resulting from environmental perturbations with uncontrolled release of inflammatory cellular contents, which is used as an assay that is complementary to the MTT cell viability assay. In this study, we utilized flow cytometric analysis for PDot-induced cellular necrosis. Necrosis as measured by Hoechst 33342 uptake (Figure 4) revealed a dose-dependent increase in cell death for both types of nanoparticles. Importantly, the cell death caused by QDot exposure is much higher than that caused by PDot exposure for all the doses tested. For example, at the 5 nM dose, the cell death with QDots was approximately 4 fold higher than that with PDots. The cell death caused by PDots is less than 5% for all the doses used, indicating that PDots do not cause significant loss of cell membrane integrity, which is consistent with the outcomes obtained from the aforementioned MTT and Trypan blue assays. It should be noted that the level of cell death caused by both types of nanoparticle was less than 10% necrosis at the highest dose (40 nM).

5. Cell cycle analysis

The cell cycle consists of 4 stages: gap1 (G1), DNA synthesis (S), and gap2 (G2), and mitosis (M) phases. Cells with partially damaged DNA will often arrest in the G1, S, or (G2/M) phases, while those with extensive damage to DNA or those that have sustained significant mitochondrial dysfunction will undergo apoptosis, causing accumulation of cells in the subG1 compartment[26]. Cell cycle analysis, therefore, is widely used to investigate cellular behaviors such as apoptosis, cell cycle arrest, and DNA damage. Our experimental results indicated that cell cycle was not affected by PDots for any of the doses tested. The percentage of cells in the various phases of the cell cycle was similarly not affected by QDot exposures (Figure 5).

6. Measures of oxidative stress by flow cytometry

6.1 Cardiolipin oxidation as measured by NAO fluorescence—Cardiolipin exists almost exclusively in the inner mitochondrial membrane and is known to be closely linked with the mitochondrial bioenergetic machinery. A change in the oxidative state of cardiolipin is believed to be causally related to the mitochondrial switch from ATP generation to initiation of apoptosis, ultimately leading to programmed cell death[27]. Therefore, the level of cardiolipin oxidation is a key factor to evaluate regarding the cytotoxicity of nanomaterials. The fluorescent dye nonyl-acridine orange (NAO) binds cardiolipin with high affinity, thus providing a quantitative measure of lipid peroxidation in the inner mitochondrial membrane. As shown in Figure 6, both QDots and PDots caused a dose dependent increase in cardiolipin peroxidation. For example, the relative intensity of NAO fluorescence was 93% and 90% of the vehicle control for the 5 nM dose of QDots and PDots, respectively. The fact that PDot nanoparticle caused less than a 10% decrement in NAO fluorescence indicated that there was a negligible effect of PDots on peroxidation of the mitochondrial inner membrane lipid cardiolipin. As the dose increased to 40 nM, NAO fluorescence was decreased to 70% and 50% of controls for QDots and PDots, respectively. Thus, the overall cardiolipin oxidation of QDots is slightly less than that of PDots, but without significant effect for either particle type at doses less than 10 nM, and, it should be noted that in almost all known biological applications, the concentration of PDots used was in the range of 1-10 nM.

6.2 Total thiol level as measured by MBB fluorescence—Thiol compounds have very important biological functions. For example, the most abundant low molecular mass thiol, glutathione, is widely found in living cells and is involved in many biological reactions. Oxidation of thiol compounds causes their function loss, potentially damaging the living cell. The thiol level or oxidation level can be determined by MBB, a fluorescent probe, with high binding affinity to thiol, thus measuring many biologically important thiol. Figure 7 showed the thiol level in RAW264.7 cell using MBB for both QDots and PDots with dose ranging from 2.5 nM to 40 nM. The thiol level was found almost not changed among all the doses, while the total thiol showed an increasing trend with QDots treatment at higher doses. In addition, at lower dose (2.5nM to 10nM), the thiol level for PDots was higher than that of QDots. Total thiol levels were significantly increased by QDots at the highest concentration (40 nM). The results indicated that the presence of PDots does not affect the oxidation of thiol with all doses.

6.3 NAD(P)H fluorescence—The reduced nicotinamide adenine dinucleotide and the reduced nicotinamide adenine dinucleotide phosphate are noted as NAD(P)H with fluorescence emission of ~460 nm, brighter than their corresponding oxidized counterparts (NAD(P)). The fluorescence of NAD(P)H is used to evaluate the metabolic oxidation-reduction state in the mitochondria and in the cytoplasm. Figure 8 shows RAW264.7 NAD(P)H fluorescence after treatment with QDots and PDots with doses ranging from 2.5 nM to 40 nM. NAD(P)H fluorescence showed an increase at higher doses of both PDots and QDots but was much more significant for QDots (Figure 6). For example, the NAD(P)H fluorescence was 85% and 60% of controls for 5 nM dose of QDots and PDots, respectively. As the dose increased to 40 nM, the NAD(P)H fluorescence was increased to 180% and

135% of controls for QDots and PDots, respectively. This increase has several possible explanations. When the electron transport chain is compromised, the levels of NADH may increase, leading to an increase in UV excited autofluorescence. Alternatively, an increase in NADPH may occur for several reasons, including increased reduction of NADP via glucose 6-phosphate dehydrogenase, isocitrate dehydrogenase, malic enzyme, or nicotinamide adenine dinucleotide transhydrogenase activities. The exact reasons for this increase are thus complicated and beyond the scope of the current investigation.

7. Colocalization of QDots and PDots with organelles

Finally, we utilized confocal microscopy to assess the internalization and colocalization of QDots and PDots in RAW264.7 cells. Both QDots and PDots were observed to be in early endosomes, followed by lysosomes, and to a lesser extent mitochondria (Figure 9). The ratio of the percentage of nanoparticles in lysosomes vs. early endosomes is 1.9 fold higher for PDots relative to QDots, suggesting a faster progression of PDots through the endosomal compartment to the lysosomal compartment. Localization of both particle types to Golgi was negligible, although curiously it was over 2 fold higher for QDots than PDots.

Conclusions

Overall, PDots were less toxic according to the necrosis result, but did cause more cardiolipin peroxidation than Qdots at higher concentrations. However, the advantage of PDots is their fluorescence intensity, which was 10 fold higher at 10 nM than that of QDots in our cellular uptake studies. This would allow one to use a lower concentration of PDots with little to no effect on toxicity or oxidative stress. Specifically, PDots showed higher total thiol levels than that of QDots at the lower dose levels (2.5nM to 10nM). At higher dose levels (20 nM to 40 nM) QDots cause significantly higher thiol levels in RAW264.7 cells, than was seen with PDots, suggesting that QDots elicit compensation to oxidative stress by increasing either GSH levels or thioredoxin/thioredoxin reductase activity. NAD(P)H levels showed an initial depletion, then repletion over control at the higher concentration for QDots. PDots showed a similar trend but this was not statistically significant. Also, due to their apparently increased speed of early endosome to lysosomal localization, PDots might be expected to degrade at a faster rate. However, this was not seen, as the fluorescence of PDots remained very high after internalization. Thus, taken together the results of this investigation indicate that PDots may be the preferred nanoparticle platform when considering biomedical applications.

Acknowledgements

This work was supported by NIH grants U19ES019545 and P30ES007033, as well as R21CA186798 and R01CA175215.

References

1. Wu C, Chiu DT. Angewandte Chemie International Edition. 2013; 52:3086.
2. Zhu C, Liu L, Yang Q, Lv F, Wang S. Chemical Reviews. 2012; 112:4687. [PubMed: 22670807]
3. Li K, Liu B. Journal of Materials Chemistry. 2012; 22:1257.

4. Das S, Powe AM, Baker GA, Valle B, El-Zahab B, Sintim HO, Lowry M, Fakayode SO, McCarroll ME, Patonay G, Li M, Strongin RM, Geng ML, Warner IM. Analytical Chemistry. 2012; 84:597. [PubMed: 22050042]
5. Wu C, Schneider T, Zeigler M, Yu J, Schiro PG, Burnham DR, McNeill JD, Chiu DT. J Am.Chem. Soc. 2010; 132:15410. [PubMed: 20929226]
6. Wu C, Jin Y, Schneider T, Burnham DR, Smith PB, Chiu DT. Angew. Chem., Int. Ed. 2010; 49:9436.
7. Pecher J, Mecking S. Chemical Reviews. 2010; 110:6260. [PubMed: 20684570]
8. Wu C, Bull B, Szymanski C, Christensen K, McNeill J. ACS Nano. 2008; 2:2415. [PubMed: 19206410]
9. Wu C, Hansen SJ, Hou Q, Yu J, Zeigler M, Jin Y, Burnham DR, McNeill JD, Olson JM, Chiu DT. Angewandte Chemie International Edition. 2010; 50:3430.
10. Fernando LP, Kandel PK, Yu J, McNeill J, Ackroyd PC, Christensen KA. Biomacromolecules. 2010; 11:2675. [PubMed: 20863132]
11. Pu KY, Li K, Shi JB, Liu B. Chemistry of Materials. 2009; 21:3816.
12. Hong G, Zou Y, Antaris AL, Diao S, Wu D, Cheng K, Zhang X, Chen C, Liu B, He Y, Wu JZ, Yuan J, Zhang B, Tao Z, Fukunaga C, Dai H. Nat Commun. 2014:5.
13. Ye F, Wu C, Jin Y, Chan Y-H, Zhang X, Chiu DT. Journal of the American Chemical Society. 2011; 133:8146. [PubMed: 21548583]
14. Chan Y-H, Wu C, Ye F, Jin Y, Smith PB, Chiu DT. Analytical Chemistry. 2011; 83:1448. [PubMed: 21244093]
15. Ye F, Wu C, Jin Y, Wang M, Chan Y-H, Yu J, Sun W, Hayden S, Chiu DT. Chemical Communications. 2012; 48:1778. [PubMed: 22218705]
16. Pu K, Shuhendler AJ, Jokerst JV, Mei J, Gambhir SS, Bao Z, Rao J. Nat Nano. 2014; 9:233.
17. Sun W, Ye F, Gallina ME, Yu J, Wu C, Chiu DT. Analytical chemistry. 2013
18. Geng J, Sun C, Liu J, Liao L-D, Yuan Y, Thakor N, Wang J, Liu B. Small. 2014 DOI 10.1002/smll. 201402092.
19. Moon JH, McDaniel W, MacLean P, Hancock LF. Angewandte Chemie. 2007; 119:8371.
20. Li K, Pan J, Feng S-S, Wu AW, Pu K-Y, Liu Y, Liu B. Advanced Functional Materials. 2009; 19:3535.
21. Zhu S, Zhang J, Wang L, Song Y, Zhang G, Wang H, Yang B. Chemical Communications. 2012; 48:10889. [PubMed: 23032967]
22. Li S, Chen J, Chen G, Li Q, Sun K, Yuan Z, Qin W, Xu H, Wu C. Macromolecular Bioscience. 2014 DOI 10.1002/mabi.201400428.
23. Smith WE, Brownell J, White CC, Afsharinejad Z, Tsai J, Hu X, Polyak SJ, Gao X, Kavanagh TJ, Eaton DL. ACS Nano. 2012; 6:9475. [PubMed: 23039050]
24. McConnachie LA, White CC, Botta D, Zadworny ME, Cox DP, Beyer RP, Hu X, Eaton DL, Gao X, Kavanagh TJ. Nanotoxicology. 2013; 7:181. [PubMed: 22264017]
25. Soenen SJ, Demeester J, De Smedt SC, Braeckmans K. Biomaterials. 2012; 33:4882. [PubMed: 22494884]
26. AshaRani PV, Low Kah Mun G, Hande MP, Valiyaveettil S. ACS Nano. 2009; 3:279. [PubMed: 19236062]
27. Gonzalvez F, Gottlieb E. Apoptosis. 2007; 12:877. [PubMed: 17294083]

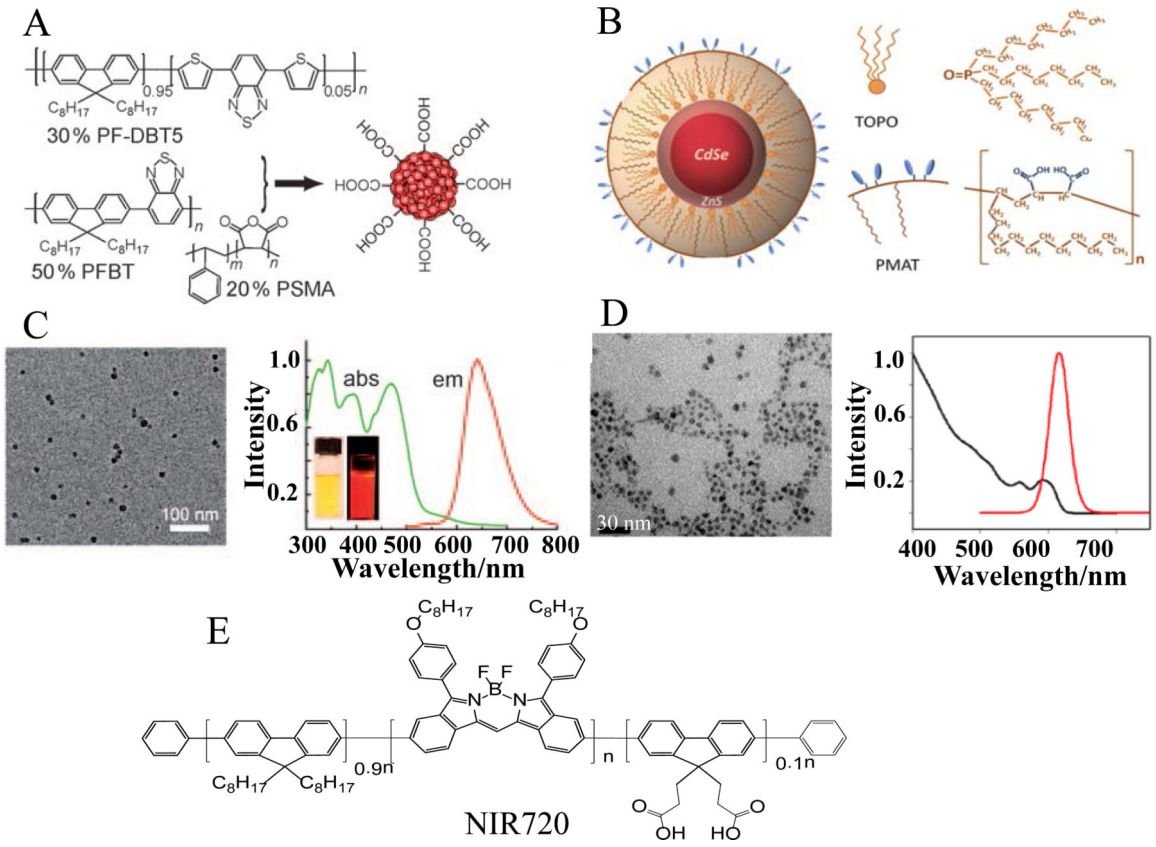

Figure 1.

PDots and QDots synthesis scheme and characterization. (A). Red PDots (PFBT/PFDBT5) (B) QDot preparation and schematic of their structural characteristics. (C) PDot and (D) QDot size determination from TEM and dynamic light scattering properties,[9,24] (E) Structure of NIR720.

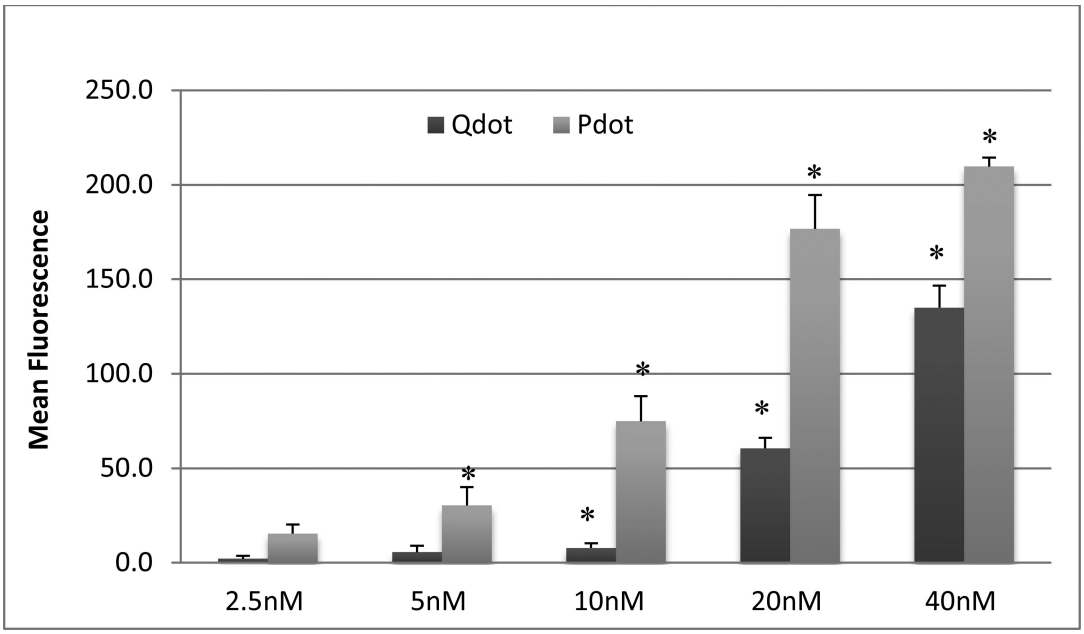

Figure 2.

Updake of PDots and QDots by Raw264.7 cells. The uptake of nanoparticles was measured by flow cytometry. The mean fluorescence intensity of each cell was evaluated as a means to qualitatively determine nanoparticle uptake. *Statistically significant by 2-way ANOVA and Student t-test for dose effect.

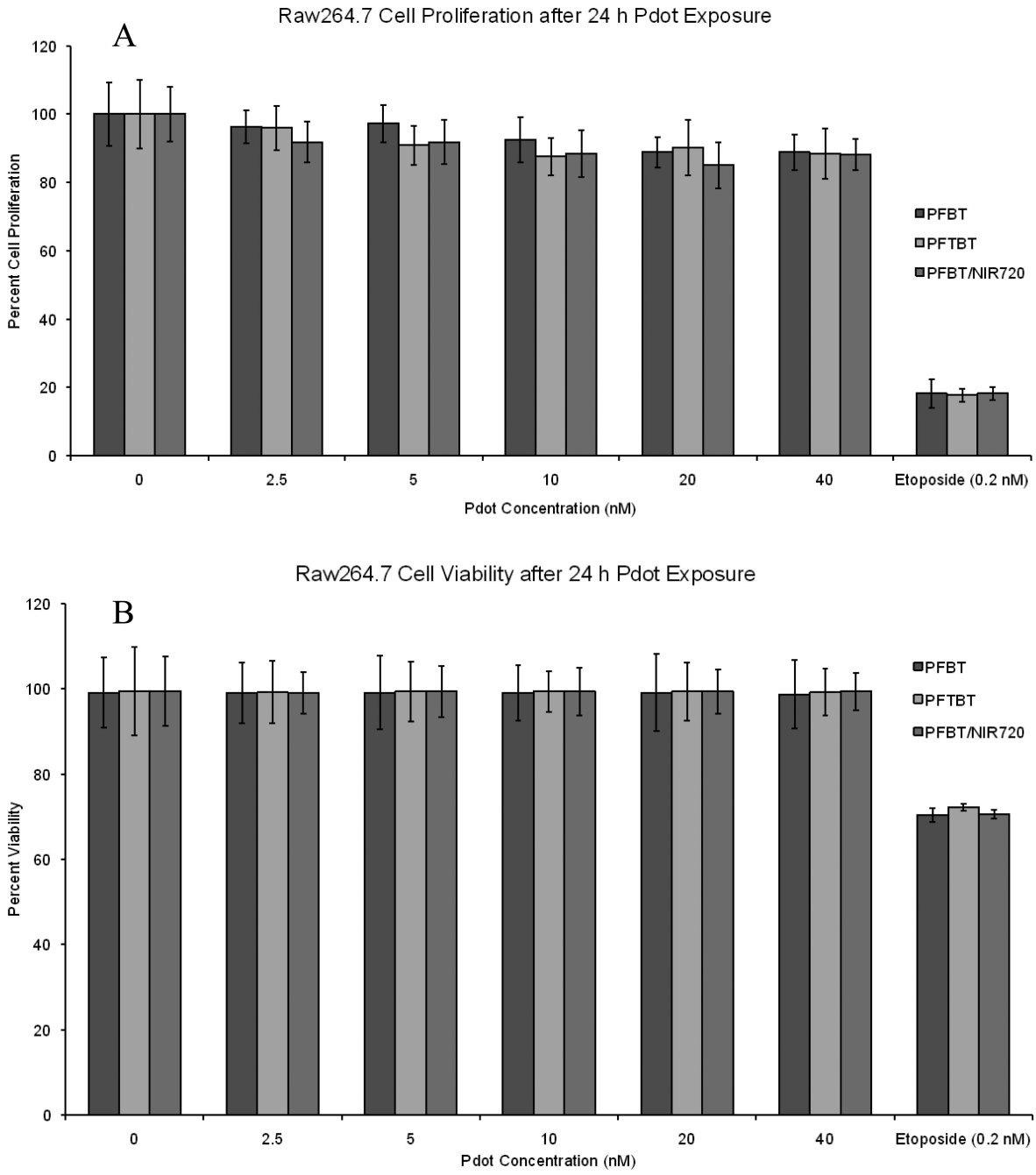

Figure 3.

The effect of PDot and QDot treatment on cellular viability using (A) MTT reduction and (B) Trypan Blue exclusion assays.

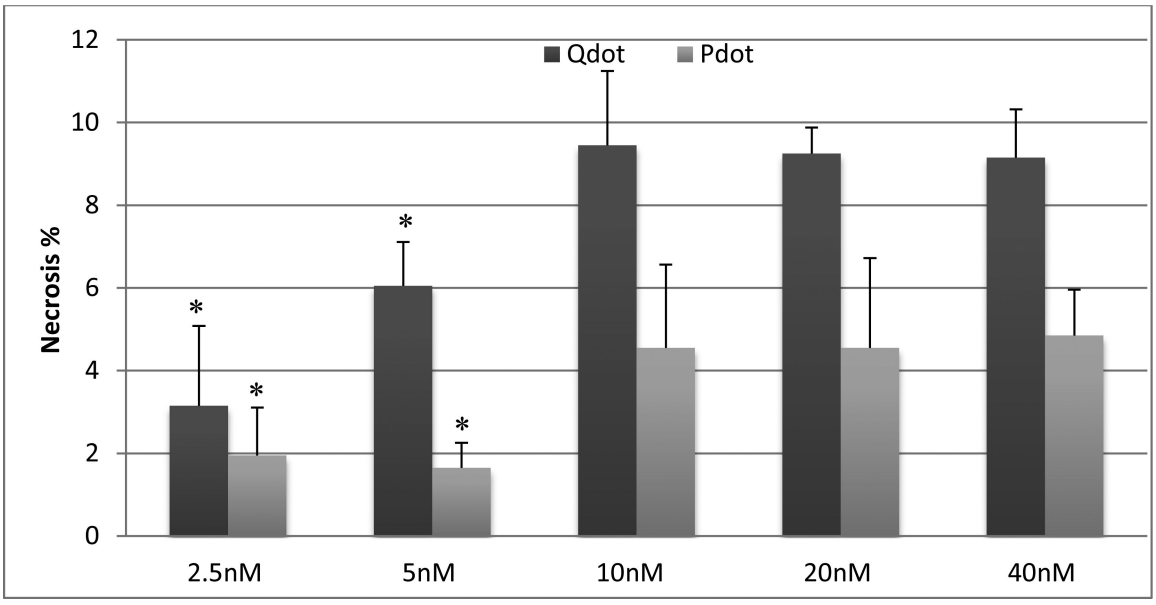

Figure 4.
Effects of QDots and PDots on necrosis (cell death) in RAW264.7 cells.

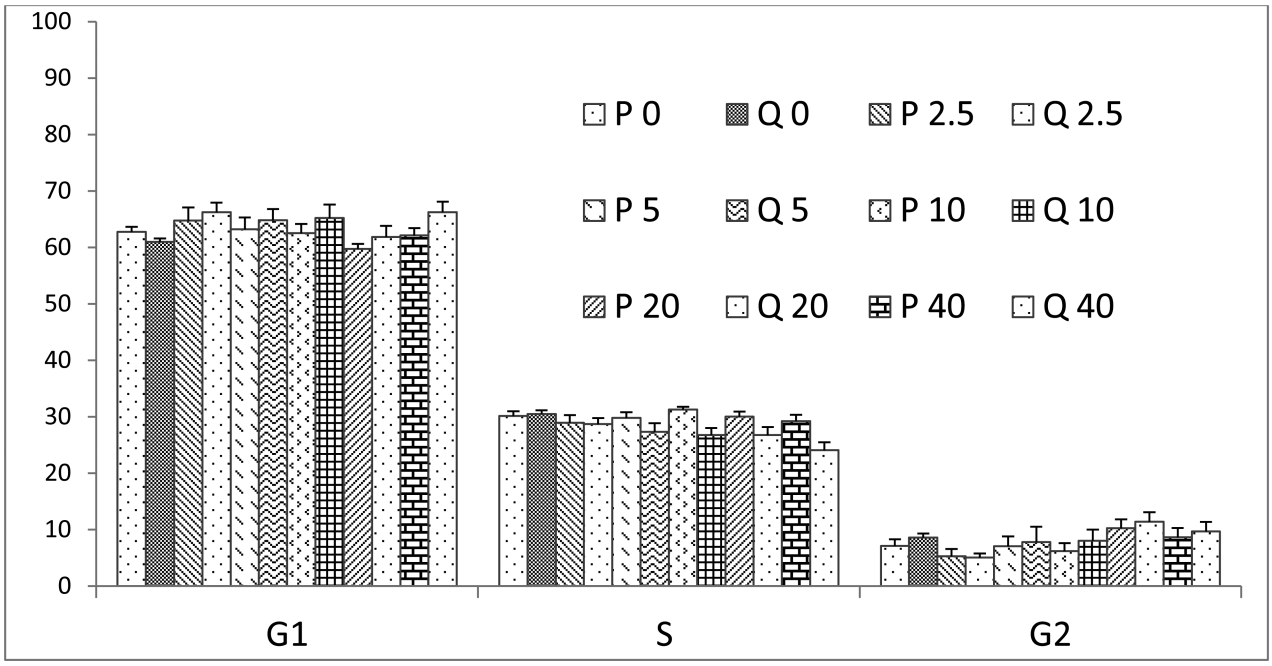

Figure 5.

Cell cycle analysis by flow cytometry. P0, P2.5, P5, P10, P20, P40 and Q0, Q2.5, Q5, Q10, Q20, Q40 represent PDot and QDot with 0, 2.5, 5, 10, 20 and 40 nM concentration, respectively.

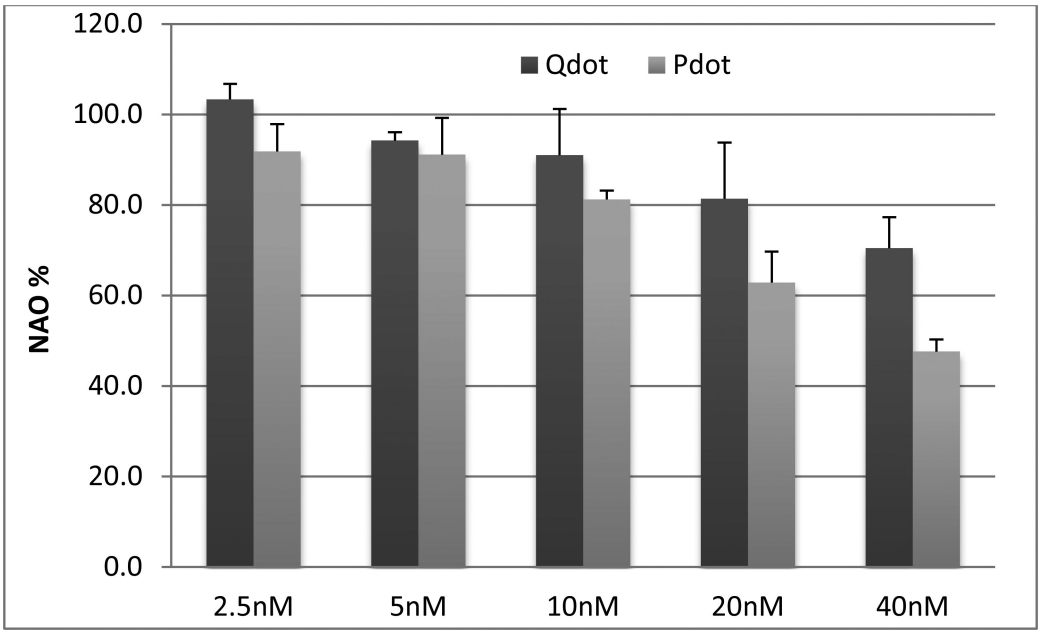

Figure 6.

Effects of QDots and PDots on mitochondrial cardiolipin oxidation in RAW264.7 cells as indicated by diminution in NAO fluorescence. *Statistically significant by 2-way ANOVA and Student t-test for dose effect.

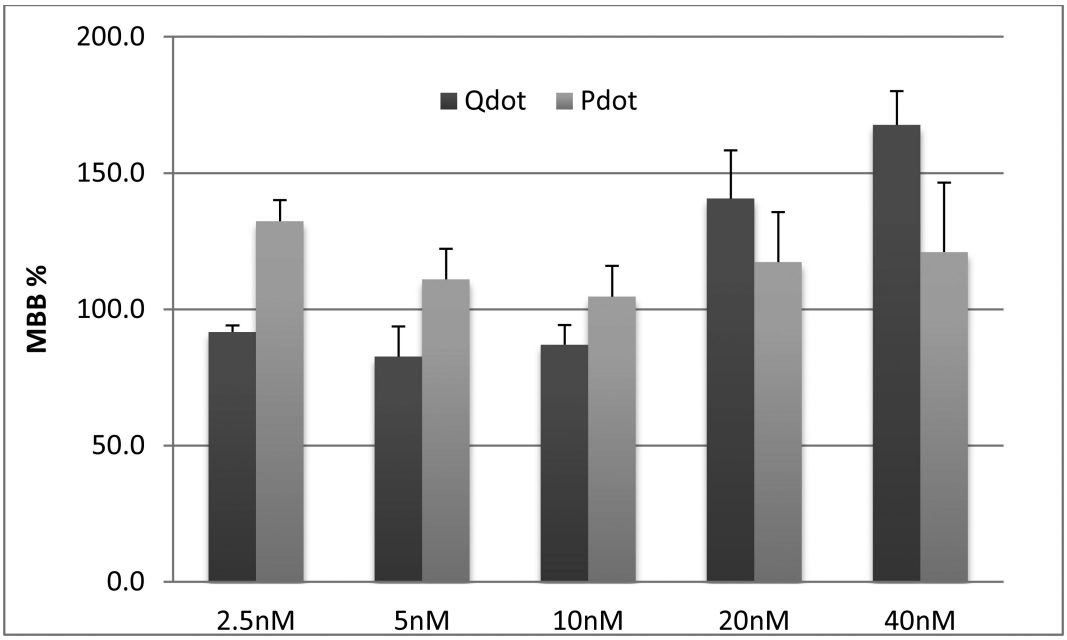

Figure 7.
Effects of QDots and PDots on total thiols in RAW264.7 cells as indicated by MBB fluorescence.

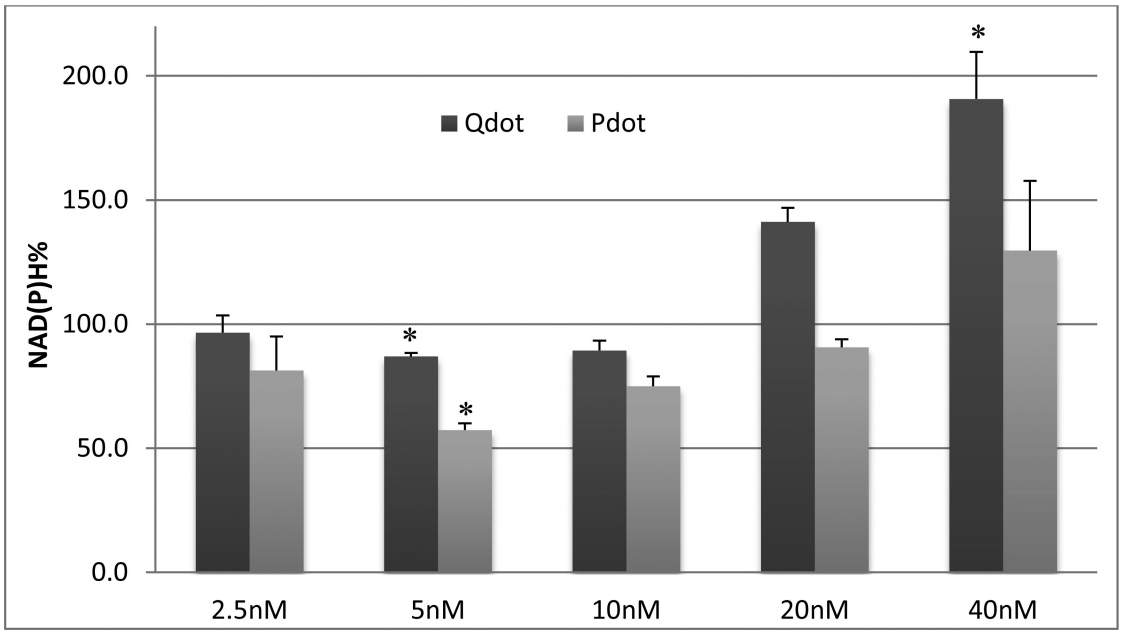

Figure 8.

Effects of QDots and PDots on NAD(P)H content in RAW264.7 cells as indicated by UV light excited blue autofluorescence. *Statistically significant by 2-way ANOVA and Student t-test for dose effect.

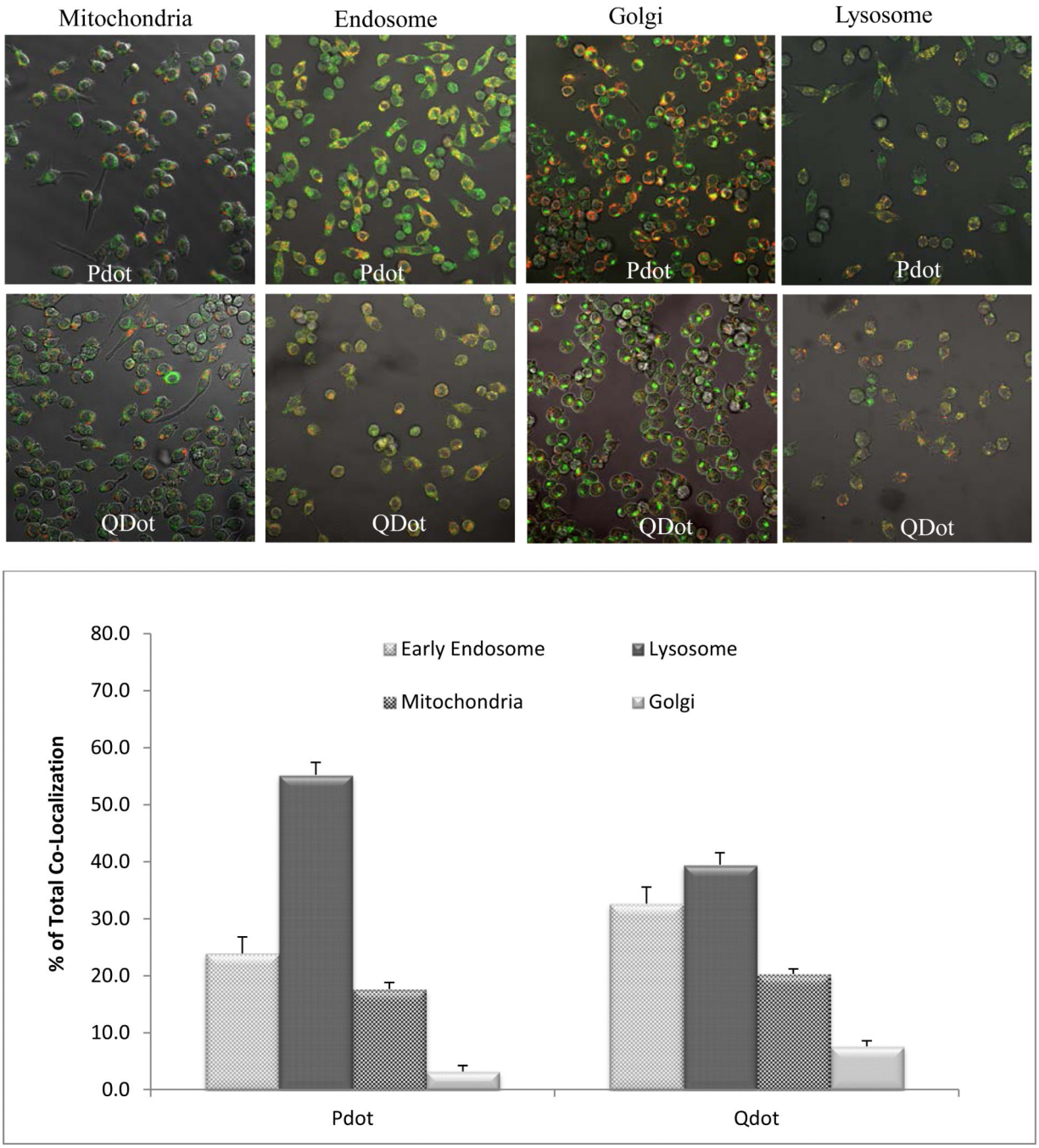

Figure 9.

Colocalization of QDots and PDots with subcellular organelles in RAW264.7 cells. Green color represents organelle stain; yellow color represents Pdot/Qdot stain.